ground water

Modeling the Transient Response of Saline Intrusion to Rising Sea-Levels

by Matt D. Webb[1] and Ken W.F. Howard[2]

Abstract

Sea levels are expected to rise as a result of global temperature increases, one implication of which is the potential exacerbation of sea water intrusion into coastal aquifers. Given that approximately 70% of the world's population resides in coastal regions, it is imperative to understand the interaction between fresh groundwater and sea water intrusion in order to best manage available resources. For this study, controlled investigation has been carried out concerning the temporal variation in sea water intrusion as a result of rising sea levels. A series of fixed inland head two-dimensional sea water intrusion models were developed with SEAWAT in order to assess the impact of rising sea levels on the transient migration of saline intrusion in coastal aquifers under a range of hydrogeological property conditions. A wide range of responses were observed for typical hydrogeological parameter values. Systems with a high ratio of hydraulic conductivity to recharge and high effective porosity lagged behind the equilibrium sea water toe positions during sea-level rise, often by many hundreds of meters, and frequently taking several centuries to equilibrate following a cease in sea-level rise. Systems with a low ratio of hydraulic conductivity to recharge and low effective porosity did not develop such a large degree of disequilibrium and generally stabilized within decades following a cease in sea-level rise. This study provides qualitative initial estimates for the expected rate of intrusion and predicted degree of disequilibrium generated by sea-level rise for a range of hydrogeological parameter values.

Introduction

Water supply issues are an essential aspect in the development and sustainability of societies. Given that approximately 70% of the world's population resides in coastal regions, it is imperative to understand the interaction between fresh groundwater and sea water intrusion in order to best manage available resources (Bear et al. 1999). Densely populated arid and semi-arid zones are often particularly vulnerable as a result of high demand and limited resources leading to intensive groundwater extraction (FAO 1997; Cameo 2006). Examples include coastal aquifers in Egypt and India (Sherif and Singh 1999), Tunisia (Paniconi et al. 2001), Mexico (Steinich et al. 1998), the Gaza Strip (Yakirevich et al. 1998), and Argentina (Martínez and Bocanegra 2002).

An additional factor in the need to understand this system is the current scientific opinion that sea levels are expected to continue to rise as a result of climate change (IPCC 2008). The processes responsible for this include changes in atmospheric pressure, thermal expansion of oceans, and melting ice caps and glaciers (Meehl et al. 2005). The Intergovernmental Panel on Climate Change (IPCC 2001) estimates that by 2100 a global sea-level rise of between 0.09 and 0.88 m will have occurred. Assuming that all other parameters remain constant, it logically follows that a fresh water/saline interface would shift inland as a result of an increase in sea water head.

This concept is explored analytically for two-dimensional (2D) unconfined coastal aquifers by Werner

[1]Corresponding author: School of Geography, Earth and Environmental Sciences, University of Birmingham, Birmingham B15 2TT, UK; m.webb@bhamalumni.org

[2]Groundwater Research Group, University of Toronto, 1265 Military Trail, Scarborough, Ontario M1C 1A4, Canada.

Received November 2009, accepted August 2010.

doi: 10.1111/j.1745-6584.2010.00758.x

and Simmons (2009), where first-order assessments are made of the changes in sea water intrusion due to rises in sea level. The limitations imposed by such an approach include the Dupuit–Forchheimer approximation (horizontal flow), no mixing between the fresh and salt waters, no seepage face at the coast, homogeneous and isotropic hydraulic properties, and only under steady-state conditions (Custodio 1987b). Such assumptions may be suitable in particularly simple systems, but will affect the accuracy of the output to varying degrees and in some cases may result in highly inaccurate estimations. As recognized by Werner and Simmons (2009), there is a surprising lack of quantitative analysis regarding the estimated extent of intrusion for any particular set of hydrogeological parameters as sea-levels rise.

An additional limitation of the analytical approach is that no consideration is given to transient behavior. Current understanding regarding the period of time between two dynamic equilibria is relatively vague, with estimates ranging from decades to centuries (FAO 1997) with no systematic method to make reasonable estimates. In this article, we aim to numerically model the same 2D unconfined coastal aquifer system investigated by Werner and Simmons (2009) in an effort to relax the number and severity of the constraints imposed by the assumptions required for analytical analysis, and to investigate the behavior of the coastal system between the two steady states determined by their research.

Werner and Gallagher (2006) numerically modeled the coastal region of the Pioneer Valley in northern Queensland and suggested that the system is most likely not in equilibrium and is unlikely to stabilize due to variations in land use and climatic conditions. Hughes et al. (2009) recognized that several studies of coastal regions indicated that chloride concentration distributions are often in a state of disequilibrium with current sea levels. However, relatively rapid response of chloride distributions to changes in sea level may occur under certain conditions, for example, the highly permeable Dutch coastal aquifer system was likely to have become salinated within decades (Post and Kooi 2003). The fact that the rate of chloride concentration response to changes in sea level appears to vary significantly between different aquifers highlights how important it is to be able to understand the relative significance and effect of the hydrogeological parameters involved.

Groundwater flow in coastal aquifers is generally controlled by anthropogenic effects, hydraulic gradients, chloride concentration, and temperature. Recharge, discharge, and aquifer properties and dimensions determine the gradients (Hughes et al. 2009). The importance of these properties can be systematically analyzed in terms of output which has some practical implication (e.g., migration of intrusion interface, time to establish a new dynamic equilibrium, etc.). However, with the increased scope of output data in numerical modeling, additional complications are introduced. For instance, hydrodynamic dispersion must be taken into account; the resulting mixing zone implies that a range of concentrations will be present in the system. The acceptable salinity level of drinking water is often taken to be less than 250 mg/L (Choi and Lee 2007). The Unites States Environmental Protection Agency (2009) recommends maximum contaminant levels for chloride in public water systems of 250 mg/L; the same target is used in Canada. Higher levels result in undesirable taste and potential corrosion to the distribution systems (Health Canada 1979).

Complications such as tidal effects, heterogeneity, variable recharge, and unsaturated effects are generally less well understood (Cameo 2006), and in an effort to constrain the research these will not be considered in this study. Although site-specific studies have obvious advantages for groundwater management for that particular area, the geological complexity may obscure a detailed investigation into the relative importance of the hydrogeological parameters and aquifer geometry, and hence would limit the transferability of the results. Post (2005) suggests that the main concern with numerical modeling of coastal aquifer systems is the need to better characterize the model input parameters. Given the complexity of the systems involved, a constrained parametric study may provide us with the platform to make qualitative estimates regarding the potential hydrogeological behavior of a particular aquifer system. It is worth noting that in certain specific situations there may actually be beneficial aspects to sea water intrusion (Howard 1987). In this study, we will assume that additional salinization of an aquifer is not a desirable outcome.

Climate Change Predictions

Recent projections of sea-level rise vary and no consensus has been reached. The IPCC (2001) predicted that by 2100 global sea levels would rise between 0.09 and 0.88 m for the Special Report on Emissions Scenarios (Church et al. 2001). An alternate estimate proposed a global-average sea-level rise of between 0.11 and 0.77 m from 1990 to 2100, which included melting permafrost and ice sheets, and sediment deposition, and also reflected the inherent uncertainties in modeling (Church et al. 2001). IPCC (2008) suggested that sea-level rise may be in the order of 0.18 to 0.59 m for the same timescale, but pointed out that the projections do not include either uncertainties in future rapid changes in ice disintegration and flow or climate-carbon feedback scenarios; hence the upper value should not to be considered to be the maximum expected sea-level rise by 2100. Rahmstorf (2007) developed a semi-empirical relationship that connected sea-level rise to global mean surface temperature. When applied to warming patterns estimated by the IPCC, a sea-level rise of 0.5 to 1.4 m was predicted. However, some researchers suggest that current predictions are too conservative. Hansen (2007) proposed that a scientific reticence serves to diminish estimates and that system inertias could result in changes far beyond current predictions. Woodworth et al. (2009) commented on the historical existence of nonlinear trends in rates of change of sea levels.

Model and Application

Werner and Simmons (2009) tested two conceptual models which represent the likely range of behavior in the field. The lower bound expected for saline intrusion is characterized by a flux-controlled system, where the groundwater discharge to the sea is constant (i.e., hydraulic gradients are maintained during sea-level rise by a corresponding increase in groundwater level). The upper bound is represented by head-controlled systems, where the inland head boundary is assumed to remain constant due to the presence of hydrogeological controls such as surface water bodies or well fields (Werner and Simmons 2009).

Groundwater discharge to the sea is an inexact figure because direct measurements can rarely be taken. An estimate is often obtained from the residual term in the mass balance equation, which contains the accumulated errors. The resulting figure is usually relatively small compared to the other terms in the equation and is not reliable (Custodio 1987a). Given that the flux-controlled case provides the lower bound of expected sea water intrusion, the true extent of salinity migration is likely to be greater, hence reducing the decision-making value of that conceptual model. For the reasons aforementioned, in particular the greater importance in estimating the upper bound of sea water intrusion, we have opted only to analyze the head-controlled system.

Werner and Simmons (2009) investigated the analytical steady-state conditions of saline intrusion for a range of sea-level rise scenarios in a shallow unconfined alluvial aquifer. Parameter values were based on an earlier study concerning sea water intrusion in the Pioneer Valley, Australia (Werner and Gallagher 2006). For the purposes of comparability between the numerical output and analytical solutions for the head-controlled system, we will use the same baseline and range of sea-level rise used by Werner and Simmons (2009), that is, up to 1.5-m sea-level rise with the baseline value equal to the upper bound proposed by the IPCC (2001) of 0.88 m. The conceptual model for the head-controlled model is shown in Figure 1, parameters and model dimensions retain the labels designated in Werner and Simmons' (2009) analytical analysis.

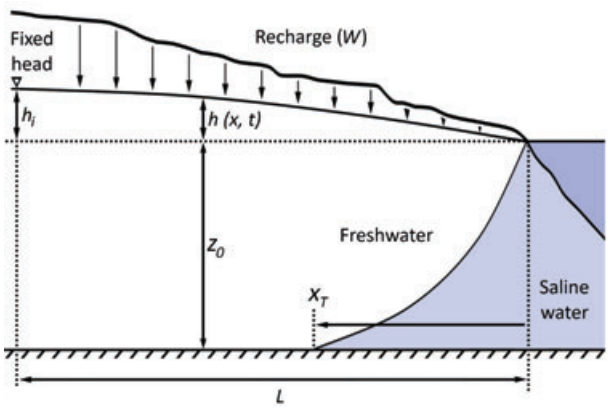

Figure 1. Conceptual model of a coastal aquifer controlled by an inland fixed-head (h_i).

For the purposes of our investigation, a series of transient 2D numerical finite difference model equivalents of the analytical steady-state solutions were produced with the US Geological Survey program SEAWAT Version 4 (Langevin et al. 2008). This combines MODFLOW 2000 (Harbaugh et al. 2000) and MT3DMS (Zheng and Wang 1999) for groundwater flow and solute transport, respectively. Detailed descriptions of the numerical methods and equations used in SEAWAT can be found in Guo and Langevin (2002) and Langevin et al. (2008).

We know that when the ocean head rises, so does the saline intrusion. However, without investigation we have no general indicator of the degree of disequilibrium inherent in a system at any given point in time. This is important for groundwater management because lack of knowledge regarding the potential additional sea water intrusion under current hydrological conditions may result in an abstraction regime with unexpected extensive sea water pollution of the aquifer system many years in the future. For this reason the investigation has an emphasis on the behavior of the extent of intrusion after 90 years of gradual sea-level rise, after which the boundary conditions will be assumed stable, so that it is possible to evaluate how a range of hydrogeological parameters are likely to affect the state of disequilibrium generated over the course of the change in sea level.

The output was used to evaluate the transient behavior of the systems for a range of parameter sets, in order to estimate the extent of the intrusion following the sea-level rise conditions, and to approximate the length of time to a state of dynamic equilibrium. Theoretically, the transitional period between two dynamic equilibria will be nonfinite, and in reality the long-term changes in climate, and even geological and geomorphological processes, will result in an ever changing system (FAO 1997). For simplicity, we assume that a dynamic equilibrium occurs when the position of the saline toe reaches a steady state to the nearest 0.1 m during the course of the 750-year model duration.

Given that the numerical models of coastal aquifer systems include dispersion, it is necessary to specify a particular concentration within the mixing zone which represents the maximum extent of the intrusion x_T at any point in time (shown as the position of the saline water toe in Figure 1). Custodio (1987b) defined the mixing zone as the surfaces corresponding to 1% and 95% sea water content based on either total dissolved solids (TDS) or chloride content, or alternatively the lower value may be chosen as the maximum TDS or chloride concentration for drinking water standards. Taking into account the drinking water standards discussed earlier, a lower salinity concentration limit of 250 mg/L was used to estimate the maximum extent of the intrusion x_T. The 50% salinity line (17,500 mg/L) was also considered for comparison and to provide some indication of the horizontal width of the mixing zone at x_T. It should be noted that the difference between the data compiled using 250 and 17,500 mg/L

contours in terms of transient behavior and equilibrium position of x_T was minimal, and identical conclusions would be made using either set of data.

It is recognized that, in cases where the depth of the modeled aquifer is increased beyond the maximum interface depth permitted by the Ghyben–Herzberg relationship, a fresh water lens rather than a saline wedge would occur. For data interpretation in scenarios producing a fresh water lens, the definition of x_T would need to be altered, for example, taking x_T as the extent of intrusion at a particular depth. In order to avoid this complication, the aquifer depth below sea level was set equal to the baseline value of 30 m used by Werner and Simmons (2009); this ensured that the range of scenarios tested would theoretically result in a saline wedge.

In order to more closely replicate the behavior of rising sea levels, the constant head boundary conditions defined at the coast were increased linearly from the beginning of the model ($t = 0$ years) up to $t = 90$ years, from 0 m to the specified value for that parameter set. For the purposes of monitoring the disequilibrium generated by the preceding 90 years of sea-level rise, boundary conditions were held constant for the remainder of the model duration. The boundary conditions at the coast are defined as Dirichlet (type I), so that rising sea levels can be specified at all times (Guo and Langevin 2002). This introduces some loss of accuracy, particularly near the coast, as described by Padilla and Cruz-Sanjulián (1997). However, given that we are interested in the farthest point of intrusion inland, this inaccuracy may be acceptable.

The analytical solutions presented by Werner and Simmons (2009) assumed no outflow face, so in order to minimize the conceptual differences between the analytical and numerical solutions the aquifer beyond the coastal boundary has not been modeled. It is expected that inclusion of an outflow face in the model would result in a slightly increased depth to interface and reduction in the position of x_T (Fetter 2001). It was also assumed that the location of the surface coastal boundary is stationary, that is, sea water does not encroach inland during sea-level rise. This may be an acceptable assumption in cases where coastal inclination is steep; however, in regions with very shallow surface gradients a small rise in sea level may result in a large movement inland of the sea boundary.

The model has 20 layers and a column spacing of 5 m throughout the saline intrusion region. The sensitivity of the solutions to model parameters were analyzed by comparing results to those with different horizontal grid discretization, number of layers, and time-stepping schemes. The differences generated by further refinement of these factors were deemed nonsignificant relative to the effect of the hydrogeological parameters for the baseline model and would not have altered the conclusions drawn from the data. Figure 2 illustrates the dimensions and boundary conditions of the model.

The reference sea water density required to reproduce the Ghyben–Herzberg ratio (Ghyben 1888; Herzberg 1901; cited Werner and Simmons 2009) of 40:1 used

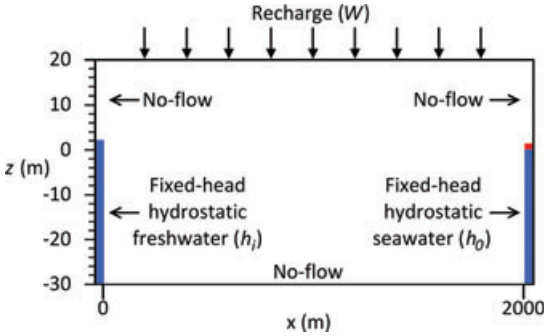

Figure 2. Boundary conditions and model domain. The maximum sea-level rise of 1.5 m is indicated by the red section of the fixed-head sea water boundary. Hydrogeological parameter values are given in Table 1.

in Werner and Simmons (2009) is a sea water density (ρ_s) of 1025 kg/m^3. Using the equation in Fofonoff (1985), the range of corresponding sea water salinity concentrations for water temperatures of 0 °C to 30 °C is 31,120 to 39,322 mg/L. Due to the variability in coastal temperatures, a salinity of 35,000 mg/L is assumed as used by other authors (Gotovac et al. 2001; Choi and Lee 2007). The sea water boundary represents hydrostatic conditions with a specified ρ_s of 1025 kg/m^3. The assigned head of the ocean boundary (h_0) is initially set to 0 m, which is then converted to a reference head using the specified value of ρ_s. Flow into the model at the sea boundary has a specified salinity concentration (C_s) of 35,000 mg/L, and flow into the model at the fresh water boundary is at $C_s = 0$ mg/L. There is no restriction on C_s for flow out at the sea boundary.

The model, as described earlier, was altered methodically to determine the behavior of the system under a range of conditions. The analytical solutions used in Werner and Simmons (2009) indicate that the location of x_T is the same for any constant ratio of K/W. It is also recognized from the analytical solutions that the controlling internal factor for x_T is the height of fresh water above sea level and that this is inversely proportional to K/W. Although these parameters were varied individually in order to allow comparison with the results in Werner and Simmons (2009), the results are presented in terms of K/W.

The baseline model was constructed with the same parameter values as used by Werner and Simmons (2009) (Table 1). Assuming a shallow, unconfined alluvial aquifer, literature values were determined for the additional parameters required by the numerical model, that is, dispersivity, molecular diffusion, porosity, storativity, fluid densities, sea water salinity and viscosity. The WHS solver package was selected for flow and, for efficiency, the implicit generalized conjugate gradient (GCG) solver with modified incomplete Cholesky preconditioner for transport. The advection term was solved using upstream finite differences, intermodal densities were calculated with the central-in-space algorithm, and flow and transport were coupled explicitly. The parameter

Table 1
Baseline Parameter Values

Parameter Name (units)	Label	Value
Aquifer depth below sea level (m)	z_0	30
Recharge (mm/year)	W	80
Horizontal hydraulic conductivity (m/d)	K_x	10
Vertical hydraulic conductivity (m/d)	K_z	10
Inland fixed-head (m.a.s.l.)	h_i	2
Model length (m)	L	2000
Longitudinal dispersivity (m)	α_L	2.5
Vertical dispersivity (m)	α_V	0.025
Molecular diffusion (m^2/d)	D	8.64×10^{-5}
Effective porosity (—)	n_e	0.32
Specific yield (—)	S_y	0.26
Specific storage (per m)	S_s	6.00×10^{-4}
Sea-level rise (m)	Δh_0	0.88
Fresh water density (kg/m^3)	ρ_f	1000
Sea water density (kg/m^3)	ρ_s	1025
Sea water salinity (mg/L)	—	35,000
Reference viscosity (kg/m d)	—	86.4
Change in viscosity over salinity (m^2/d)	—	1.92×10^{-6}
Change in density over salinity (—)	—	0.7142857
WHS solver package		
Maximum outer iterations	—	500
Maximum inner iterations	—	250
Head change criterion (m)	—	1×10^{-6}
Residual criterion	—	10
Damping factor	—	1
Relative residual criterion	—	0
Implicit GCG solver package		
Maximum outer iterations	—	1
Maximum inner iterations	—	50
Initial time step (d)	—	0.005
Maximum time step (d)	—	[1]
Multiplier	—	1.05
Relative convergence criterion	—	0.0001

[1] Set to ensure courant number < 0.75.

settings are indicated in Table 1, with default SEAWAT values assigned to any parameters not listed.

As a measure to reduce computational expense, the effect of temperature on fluid density is not considered. The following results are for variable-density flow in which the fluid density is a function of the salinity. For each model, the salinity concentration distributions prior to sea-level rise ($t = 0$ years) were re-imported as necessary for the initial values to provide stable starting conditions.

Results

The model tested the sensitivity of a range of important outputs to a variety of different parameter sets. Particular attention is given to the numerical results concerning the movement trends and position of x_T after a given number of years. Unless specified otherwise isotropy and homogeneity are assumed, with parameters taking the values shown in Table 1 and all graphical output referring to numerical rather than analytical results. Numerical results for x_T were determined by the location of the 250 mg/L salinity line. Given that specific yield (S_y) and effective porosity (n_e) are independent parameters in the groundwater flow and transport modeling equations, they have been analyzed separately. However, it is recognized that in practice these two parameters are related (McWhorter and Sunada 1977; Kasenow 2006).

Figure 3 illustrates the modeled salinity distributions for the baseline parameter set (with a sea-level rise of 1.5 m) at three key points in time: (a) equilibrium initial conditions; (b) at $t = 90$ years following 1.5 m sea-level rise; and (c) the new dynamic equilibrium salinity distribution achieved by $t = 390$ years after the sea level remained at a constant 1.5 m. x_T increases by approximately 170 m between $t = 0$ and 90 years, although the sea-levels rise; however, it is apparent from (c) that the system had developed a state of disequilibrium by $t = 90$ years because x_T increases by a further 138 m

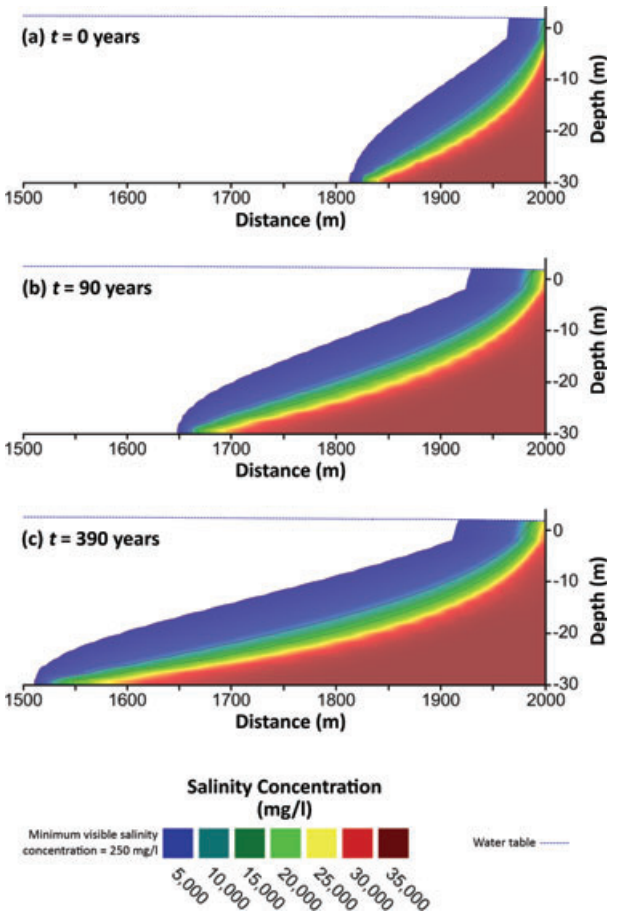

Figure 3. Salinity concentration profiles for the baseline parameter set. (a) $t = 0$ years, (b) $t = 90$ years following 1.5 m sea-level rise, and (c) new dynamic equilibrium at $t = 390$ years after boundary conditions held constant.

after this time despite boundary conditions being held constant.

Figure 4 shows the evolution of the saline intrusion between $t = 0$ and 90 years for a range of effective porosity values (n_e). The boundary conditions were held constant from $t = 90$ years onwards. With $n_e = 0.05$ and a sea-level rise of 1.5 m, the model failed to converge, for this reason a sea-level rise of 1.22 m is used for all n_e values. The difference in final interface positions for the n_e range of 0.05 to 0.46 is less than 10 m. However, the difference in transient behavior is significant. The scenario with $n_e = 0.05$ resulted in an interface position only 10.8 m from the final equilibrium position at $t = 90$ years, taking approximately 10 years to stabilize. For otherwise identical conditions, the system with $n_e = 0.46$ had an interface position of 73.0 m less than the final equilibrium position at $t = 90$ years, and took approximately 190 years to stabilize. The crosses represent the positions of x_T for the baseline parameter set if the sea-level rise ceased at that point in time and the model was given sufficient time to reach a new equilibrium. This suggests that as n_e approaches zero, the transient location of x_T tends toward the equilibrium position expected at that time if the sea-level rise ceased. The slight oscillations visible are the result of grid refinement constraints.

Figure 5 shows the position of x_T under steady-state boundary conditions, for the baseline parameter set, following a range of sea-level rise scenarios which occurred between $t = 0$ and 90 years. The difference in the position of x_T after a sea-level rise of 0.1 and 1.5 m is 159.7 m; this increases to 297.6 m over the course of 250 years. The time to equilibrium is significantly longer for the larger sea-level rise scenarios. For a sea-level rise of 0.1 m, it took just 4 years for the interface to stabilize an additional 0.2 m inland, whereas for a sea-level rise of 1.5 m it took approximately 250 years for the interface to stabilize a further 138.1 m inland.

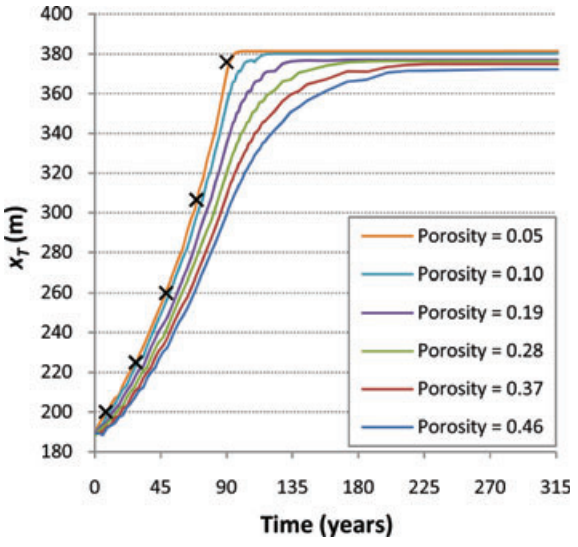

Figure 4. Position of x_T during a sea-level rise of 1.22 m (between $t = 0$ and 90 years) followed by constant boundary conditions for a range of n_e values. The crosses represent the baseline parameter set equilibrium positions of x_T if the sea-level rise ceased at that point in time.

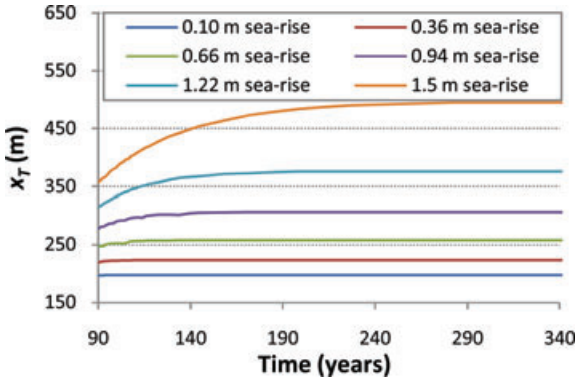

Figure 5. Position of x_T after $t = 90$ years following a range of sea-level rises between $t = 0$ and 90 years for the baseline parameter set (Table 1).

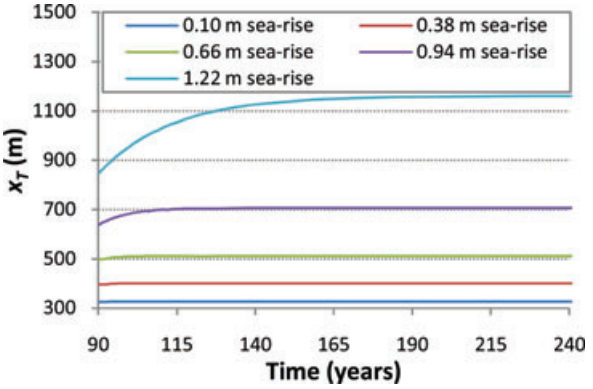

Figure 6. Position of x_T after $t = 90$ years following a range of sea-level rises between $t = 0$ and 90 years with $K/W = 4.6 \times 10^5$.

Figure 6 shows the position of x_T for a system with a K/W ratio of 4.6×10^5 under conditions otherwise identical to Figure 5. Note that there are no data included for a sea-level rise of 1.5 m as the sea water intruded the entire length of the model. By comparing the position of x_T at equilibrium in Figure 5 ($K/W = 4.6 \times 10^4$) and Figure 6, we can see that the difference with a sea-level rise of 1.22 m is approximately 785 m, and the difference with a sea-level rise of 0.1 m is close to 130 m.

In order to provide an additional comparison between the transient behavior of the data presented in Figures 5 and 6 and to evaluate the degree of disequilibrium after a given sea-level rise, we can consider the average velocity of the intrusion shown in Figure 7 for a range of K/W values and sea-level rise predictions. Given that the progression of x_T should asymptotically approach the final equilibrium position, the average velocity was calculated using the time taken to achieve 95% of the total Δx_T. The system with $K/W = 4.6 \times 10^3$ shows minimal interface movement after $t = 90$ years for any of the tested sea-level rise scenarios, in some cases a

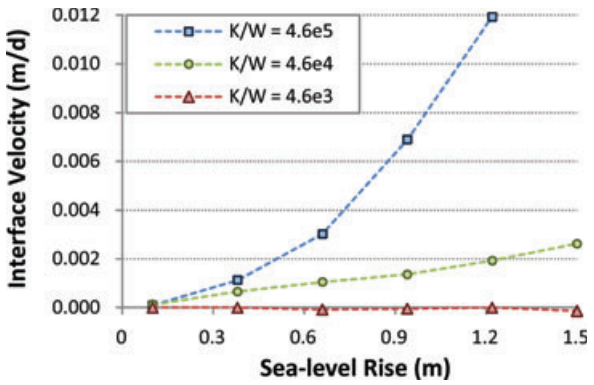

Figure 7. Average velocity of x_T inland from $t = 90$ years to 95% of total Δx_T for a range of K/W values and sea-level rises.

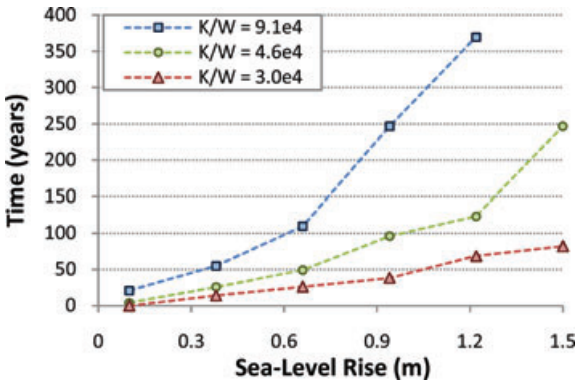

Figure 8. Approximate time to equilibrium after $t = 90$ years for a range of K/W values and sea-level rises.

negative average velocity (i.e., seaward) indicates an overall marginal retreat in interface position; however, this may be as a result of numerical inaccuracies rather than any naturally occurring physical process. Both the $K/W = 4.6 \times 10^4$ and $K/W = 4.6 \times 10^5$ systems show a positive average velocity (i.e., inland) after $t = 90$ years for the range of tested sea-level rises. The effect of the magnitude of sea-level rise on the interface velocity for a particular parameter set becomes progressively more nonlinear as K/W is increased.

Figure 8 illustrates the approximate time to equilibrium for three K/W values. The system with $K/W = 3.0 \times 10^4$ resulted in no measureable change in the position of x_T following a sea-level rise of 0.1 m, whereas it took 82 years for x_T to stabilize following a sea-level rise of 1.5 m. For $K/W = 9.1 \times 10^4$, the system took 20 years to reach a new equilibrium for a sea-level rise of 0.1 m, and 370 years for a sea-level rise of 1.22 m (note: for this parameter set a sea-level rise of 1.5 m resulted in saline water flooding the entire model). The effect of the magnitude of sea-level rise on the time to equilibrium becomes increasingly nonlinear as K/W is increased.

Figure 9a shows the change in the position of x_T (i.e., Δx_T) between $t = 0$ and 90 years for a range of S_y values, and Figure 9b shows the additional Δx_T up to the new equilibrium positions of x_T. Over the 90 years of sea-level rise, the entire range of physical S_y (from 0 to n_e) only resulted in a maximum difference in x_T positions of 5.1 m at the end of the sea-level rise conditions (Figure 9a). The discrepancy generated up to $t = 90$ years is reversed by $t = 117$ years for all parameter sets (Figure 9b).

Similar results can be seen for specific storage (Figures 10a and 10b). Over 90 years of sea-level rise, the range of tested specific storages (7.22×10^{-7} to 2×10^{-2} per m) only resulted in a maximum difference in x_T positions of 9.2 m at the end of the sea-level rise conditions (Figure 10a). The discrepancy generated up to $t = 90$ years is reversed between $t = 107$ and 112 years for all parameter sets (Figure 10b).

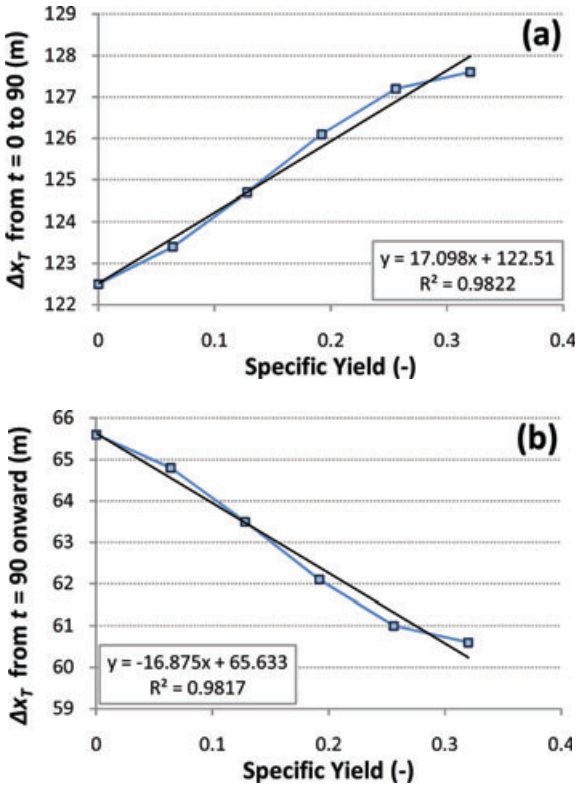

Figure 9. Δx_T for a range of S_y values. (a) $t = 0$ to 90 years and (b) $t = 90$ years onward.

Discussion

We can see from Figure 4 that n_e has a considerable effect on the responsiveness of a coastal aquifer system to changes in sea level. In general, the lower the n_e, the closer the system is to a state of dynamic equilibrium. The highest porosity systems respond relatively slowly and the salinity concentration distribution may lag behind what would be the dynamic equilibrium state by many centuries. As shown in Figure 5, a greater sea-level rise will exacerbate this effect. We can also conclude from Figure 5 that the rate of interface movements during the rising sea conditions (between $t = 0$ and 90 years) were more rapid for the higher sea-level rise scenarios, and

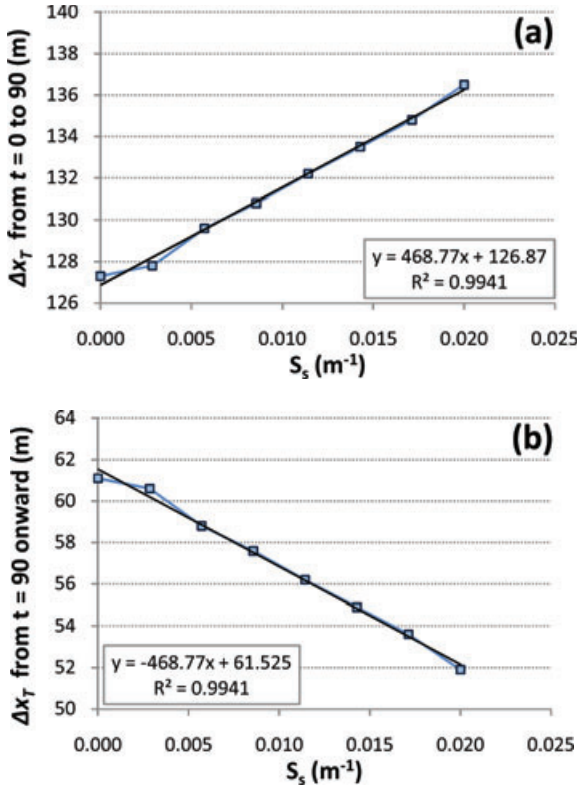

Figure 10. Δx_T for a range of S_s values. (a) $t = 0$ to 90 years and (b) $t = 90$ years onward.

also that the rate of intrusion would be elevated relative to the lower sea-level rise scenarios even if sea levels could be stabilized. Although n_e is a key parameter in the transient behavior of saline intrusion for the fixed-head model, storativity appears to play little part (Figures 9 and 10). Over a range of likely physical values (Batu 1998; Brady and Kunkel 2003) the total variation in x_T following a sea-level rise of 1.22 m over the course of 90 years was approximately only 3%. This may appear counter intuitive given the close link between n_e and S_y identified earlier. However, this behavior implies that, for the fixed-head model, the density effects and parameters driving dispersion are more important than the hydraulic response to the incremental change in ocean head.

Figures 5, 6, 7, and 8 highlight the importance of K/W, and hence the height of fresh water above sea level, with respect to the rate of intrusion during sea-level rise, additional intrusion required to establish a new dynamic equilibrium, and also the time taken to reach this state. Figure 7 indicates that the system with $K/W = 4.6 \times 10^3$ is already close to equilibrium at $t =$ 90 years following any sea-level rise in the tested range. This suggests that when monitoring the saline water distributions in an aquifer with a K/W ratio of this order, a head-controlled system may likely be in, or close to, equilibrium. However, the systems with K/W of 4.6×10^4 and 4.6×10^5 show a positive intrusion velocity over the range of tested sea-level rises. This implies that under these conditions, as a result of the sea-level rise, a degree of disequilibrium is generated in both systems.

The model with the largest tested K/W ratio (4.6×10^5) showed the largest disequilibrium in terms of additional sea water intrusion after $t = 90$ years, the largest time to equilibrium, and also the largest interface velocity. This suggests that a coastal aquifer with a high K/W might pose the most problems in terms of groundwater management. It is important to bear in mind that n_e and K, although independent properties, are indirectly related (Ahuja et al. 1989). An aquifer with high n_e may often have a high conductivity; this particular combination of properties may be particularly problematic in terms of coastal aquifer management during sea-level rise events. For otherwise constant parameters, a higher K would result in an equilibrium position of x_T further inland and a higher n_e would result in a greater degree of disequilibrium at any point in time. It is possible that an aquifer with these properties may develop a salinity distribution that could be several hundreds of meters and many centuries away from equilibrium conditions during sea-level rise. Aquifers which would traditionally be considered suitable for water supply may suffer the most in both the short and long term from sea water intrusion problems resulting from rising sea levels. Conversely, an aquifer with low K/W and low n_e is likely to show minimal response to sea-level rise and potentially reach equilibrium within a few years. The potential lack of data regarding the degree of disequilibrium in any given system may hinder our ability to develop reasonable conceptual and numerical models for site-specific analysis. Hughes et al. (2009) commented on the difficulties of numerical modeling with errors in initial heads, temperatures, and concentrations.

Conclusion

This study considered a numerical approach to the analytical work carried out by Werner and Simmons (2009) in order to allow analysis of the transient behavior of coastal aquifer systems as a result of rising sea levels. The work offers some indication of hydrogeological characteristics that may highlight regions particularly prone to either short- or long-term sea water intrusion problems. The results show that for head-controlled systems the key endogenous parameters (Δx_T during and after sea-level rise, and time to establish a new equilibrium) displayed a wide range of responses to some exogenous parameters (e.g., K, W, and n_e) with others showing relatively minimal response (S_y and S_s). The magnitude of expected intrusion, and hence the degree of disequilibrium, appears to be more relevant than storativity for predicting transient behavior when considering fixed-head models. Using the results presented, it is possible to estimate the combination of hydrogeological parameters that may result in problems with future salinity distributions.

Systems with low K/W ratio or low n_e generally did not develop a significant degree of disequilibrium and normally stabilized within decades following a cease in sea-level rise conditions. However, systems with high

K/W ratio or high n_e resulted in saline intrusion lagging behind the equilibrium sea water toe positions during sea-level rise, often by many hundreds of meters, and frequently taking several centuries to establish a new equilibrium following a cease in sea-level rise conditions. The application of these results in a practical sense will, at best, be limited to general qualitative estimates, but should improve the understanding and appreciation of the interaction between, and importance of, the individual hydrogeological parameters for head-controlled systems.

Given the large number of models needed to conduct a thorough parametric study, the resulting time constraints imposed limits on the scope of the study. Further work using parameter sets based on real-world data and numerically establishing the transient relationship between K/W and x_T may improve the applicability of the results.

There is considerable scope for additional investigation into the conceptual model design. For instance, Fujinawa et al. (2009) modeled a more complex site-specific coastal aquifer including a saline lagoon. It is possible that the insensitivity of model output to storage is a result of the fixed inland head. Further investigation into alternate boundary conditions, for example, the fixed-flux case in Werner and Simmons (2009), may help to more accurately define the effects of differing storage values. Other research may focus on, for example, modeling beyond the coast in an effort to more realistically replicate the flow regime, layered aquifers, sloping land surface resulting in landward migration of the coastal boundary, tidal effects (especially in regions with a shallow coastal gradient), transient response due to pumping, temperature effects, and aquifer depths that yield a fresh water lens as opposed to a saline wedge.

Acknowledgments

The work was supported by a Discovery Grant to K.W.F.H. from the Natural Sciences and Engineering Research Council, Canada (NSERC). We would like to thank Michael Riley for his support during the project, along with Xiaobao Li and three anonymous reviewers for their constructive comments on this paper.

References

Ahuja, L.R., D.K. Cassel, R.R. Bruce, and B.B. Barnes. 1989. Evaluation of spatial distribution of hydraulic conductivity using effective porosity data. *Soil Science* 148, no. 6: 404–411.

Batu, V. 1998. *Aquifer Hydraulics: A Comprehensive Guide to Hydrogeologic Data Analysis.* John Wiley and Sons.

Bear, J., A.H.-D. Cheng, S. Sorek, D. Ouazar, and I. Herrera. 1999. *Seawater Intrusion in Coastal Aquifers—Concepts, Methods and Practices, In Theory and Application of Transport in Porous Media.* Dordrecht, The Netherlands: Kluwer Academic Publishers.

Brady, M.M., and L.A. Kunkel. 2003. A practical technique for quantifying drainage porosity. In Proceedings of 2003 Petroleum Hydrocarbons and Organic Chemicals in Ground Water: Prevention, Assessment, and Remediation, Costa Mesa, California, 20–22 August.

Cameo, E.A. 2006. Seawater intrusion in complex geological environments. Ph.D. diss., Polytechnic University of Catalonia, Catalonia, Spain.

Choi, C.W., and J.H.M. Lee. 2007. Solving the salinity control problem in a potable water system. In *Principles and Practice of Constraint Programming—CP 2007*, LNCS 4741, ed. C. Bessiere, 33–48. Berlin/Heidelberg: Springer.

Church, J.A., J.M. Gregory, P. Huybrechts, M. Kuhn, K. Lambeck, M.T. Nhuan, D. Qin, and P.L. Woodworth. 2001. Changes in sea level. In *Climate Change 2001: The Scientific Basis*, ed. J.T. Houghton, Y. Ding, D.J. Griggs, M. Noguer, P.J. Van Der Linden, X. Dai, K. Maskell and C.A. Johnson, 639–694. New York: Cambridge University Press.

Custodio, E. 1987a. Coastal aquifers. In *Studies and Reports in Hydrology: Ground Water Problems in Coastal Areas*, chapter 2, ed. G.A. Bruggeman and E. Custodio, 6–13. Paris, France: United Nations Educational, Scientific and Cultural Organization.

Custodio, E. 1987b. Salt-fresh interrelationships under natural conditions. In *Studies and Reports in Hydrology: Ground Water Problems in Coastal Areas*, chapter 3, ed. G.A. Bruggeman and E. Custodio, 14–96. Paris, France: United Nations Educational, Scientific and Cultural Organization.

FAO. 1997. Seawater intrusion in coastal aquifers: Guidelines for study, monitoring and control. FAO Water Reports 11, 1–152. Roma, Italy: FAO.

Fetter, C.W. 2001. *Applied Hydrogeology*, 4th ed. Upper Saddle River, New Jersey: Prentice-Hall.

Fofonoff, N.P. 1985. Physical properties of seawater: A new salinity scale and equation of state for seawater. *Journal of Geophysical Research* 90, no. C2: 3332–3342.

Fujinawa, K., T. Iba, Y. Fujihara, and T. Watanabe. 2009. Modeling interaction of fluid and salt in an aquifer/lagoon system. *Ground Water* 47, no.1: 35–48. DOI:10.1111/j.1745-6584.2008.00482.x.

Ghyben, B.W. 1888. Nota in verband met de voorgenomen putboring nabij Amsterdam (Notes on the probable results of the proposed well drilling near Amsterdam). *Tijdschrift van het Koninklijk Instituut van Ingenieurs*, The Hague, 8–22.

Gotovac, H., R. Andričević, and M. Vranjes. 2001. Effects of aquifer heterogeneity on the intrusion of seawater. In Proceedings of the First International Conference on Salt Water Intrusion and Coastal Aquifers, Monitoring, Modelling and Management, Essaouira, Morocco, 23–25 April. Washington, DC: USGS.

Guo, W., and C.D. Langevin. 2002. *User's Guide to SEAWAT: A Computer Program for Simulation of Three-dimensional Variable-Density Ground-water Flow: U.S. Geological Survey Techniques of Water Resources Investigations Book 6*, chapter A7. Reston, Virginia: U.S. Geological Survey.

Hansen, J.E. 2007. Scientific reticence and sea-level rise. *Environmental Research Letters* 2: 024002.

Harbaugh, A.W., E.R. Banta, M.C. Hill, and M.G. McDonald. 2000. MODFLOW-2000, The US Geological Survey modular ground-water model—user guide to modularization concepts and the ground-water flow process. US Geological Survey, Open-File Report 00-92. Reston, Virginia: USGS.

Health Canada. 1979. Environmental and workplace health, chloride. http://www.hc-sc.gc.ca/ewh-semt/pubs/water-eau/chloride-chlorure/index-eng.php (accessed June 3, 2009).

Herzberg, A. 1901. Die Wasserversorgung einiger Nordseebder (The water supply on parts of the North Sea coast in Germany). *Journal für Gasbeleuchtung und Wasserversorgung* 44: 815–819, 824–844.

Howard, K.W.F. 1987. Beneficial aspects of sea-water intrusion. *Ground Water* 25, no. 4: 398–406. DOI:10.1111/j.1745-6584.1987.tb02144.x.

Hughes, J.D., H.L. Vacher, and W.E. Sanford. 2009. Temporal response of hydraulic head, temperature, and chloride concentrations to sea-level changes, Floridan aquifer system, USA. *Hydrogeology Journal* 17, no. 4: 793–815. DOI:10.1007/s10040-008-0412-0.

Intergovernmental Panel on Climate Change (IPCC). 2008. Climate change and water. IPCC Technical paper VI. http://www.ipcc.ch/ (accessed June 14, 2009).

Intergovernmental Panel on Climate Change (IPCC). 2001. Climate change 2001: The scientific basis. In *Contribution of Working Group I to the Third Assessment Report of the Intergovernmental Panel on Climate Change*. Cambridge, UK: Cambridge University Press. http://www.grida.no/ (accessed June 12, 2009).

Kasenow, M. 2006. *Aquifer Test Data: Analysis and Evaluation.* Water Resources Publication.

Langevin, C.D., D. Thorne, A.M. Dausman, M.C. Sukop, and W. Guo. 2008. *SEAWAT Version 4: A Computer Program for Simulation of Multi-Species Solute and Heat Transport*. U.S. Geological Survey Techniques and Methods Book 6, Chapter A22. Reston, Virginia: U.S. Geological Survey.

Martínez, D., and E. Bocanegra. 2002. Hydrogeochemistry and cation-exchange processes in the coastal aquifer of Mar Del Plata, Argentina. *Hydrogeology Journal* 10, no. 3: 393–408. DOI:10.1007/s10040-002-0195-7.

McWhorter, D.B., and D.K. Sunada. 1977. *Ground-Water Hydrology and Hydraulics.* Fort Collins, Colorado: Water Resources Publications.

Meehl, G.A., W.M. Washington, W.D. Collins, J.M. Arblaster, A. Hu, L.E. Buja, W.G. Strand, and H. Teng. 2005. How much more global warming and sea level rise? *Science* 307, no. 5716: 1769–1772. DOI:10.1126/science.1106663.

Padilla, F., and J. Cruz-Sanjulián. 1997. Modeling sea-water intrusion with open boundary conditions. *Ground Water* 35, no. 4: 704–712. DOI:10.1111/j.1745-6584.1997.tb00137.x.

Paniconi, C., I. Khlaifi, G. Lecca, A. Giacomelli, and J. Tarhouni. 2001. Modeling and analysis of seawater intrusion in the coastal aquifer of Eastern Cap-Bon, Tunisia. *Transport in Porous Media* 43, no. 1: 3–28. DOI:10.1023/A:1010600921912.

Post, V.E.A. 2005. Fresh and saline groundwater interaction in coastal aquifers: Is our technology ready for the problems ahead? *Hydrogeology Journal* 13, no. 1: 120–123. DOI:10.1007/s10040-004-0417-2.

Post, V.E.A., and H. Kooi. 2003. Rates of salinization by free convection in high-permeability sediments: Insights from numerical modelling and application to the Dutch coastal area. *Hydrogeology Journal* 11, no. 5: 549–559. DOI:10.1007/s10040-003-0271-7.

Rahmstorf, S. 2007. A semi-empirical approach to projecting future sea-level rise. *Science* 315, no. 5810: 368–370. DOI:10.1126/science.1135456.

Sherif, M.M., and V.P. Singh. 1999. Effect of climate change on sea water intrusion in coastal aquifers. *Hydrological Processes* 13, no. 8: 1277–1287.

Steinich, B., O. Escolero, and L.E. Marín. 1998. Salt water intrusion and nitrate contamination in the Valley of Hermosillo and El Sahuaral coastal aquifers, Sonora, Mexico. *Hydrogeology Journal* 6, no. 4: 518–526. DOI:10.1007/s100400050172.

United States Environmental Protection Agency. 2009. Code of Federal Regulations, Title 40, Chapter I—Environmental Protection Agency, Volume 22, Part 143.3 Secondary maximum contaminant levels. http://www.access.gpo.gov/nara/cfr/waisidx_02/40cfr143_02.html (accessed June 4, 2009).

Werner, A.D., and C.T. Simmons. 2009. Impact of sea-level rise on sea water intrusion in coastal aquifers. *Ground Water* 47, no. 2: 197–204. DOI:10.1111/j.1745-6584.2008.00535.x.

Werner, A.D., and M.R. Gallagher. 2006. Characterisation of sea-water intrusion in the Pioneer Valley, Australia using hydrochemistry and three-dimensional numerical modelling. *Hydrogeology Journal* 14, no. 8: 1452–1469. DOI:10.1007/s10040-006-0059-7.

Woodworth, P.L., N.J. White, S. Jevrejeva, S.J. Holgate, J.A. Church, and R. Gehrels. 2009. Evidence for the accelerations of sea level on multi-decade and century timescales. *International Journal of Climatology* 29, no. 6: 777–789. DOI:10.1002/joc.1771.

Yakirevich, A., A. Melloul, S. Sorek, S. Shaath, and V. Borisov. 1998. Simulation of seawater intrusion into the Khan Yunis area of the Gaza Strip coastal aquifer. *Hydrogeology Journal* 6, no. 4: 549–559. DOI:10.1007/s100400050175.

Zheng, C., and P.P. Wang. 1999. MT3DMS, A modular three-dimensional multi-species transport model for simulation of advection, dispersion and chemical reactions of contaminants in ground-water systems; documentation and user's guide. Contract Report, SERDP-99-1. Vicksburg, Mississippi: U.S. Army Engineer Research and Development Center.